

## Cation Size Effects-Modified Phase and PTCR Development in Er<sup>3+</sup> and Ca<sup>2+</sup> Co-Doped BaTiO<sub>3</sub> Ceramics During Sintering

Ronaldo Santos da Silva, Jean-Claude M'Peko\*, Lilian da Costa Fontes, Antonio Carlos Hernandes

Grupo Crescimento de Cristais e Materiais Cerâmicos – GCCMC,  
Instituto de Física de São Carlos – IFSC, Universidade de São Paulo – USP,  
CP 369, 13560-970 São Carlos - SP, Brazil

Received: October 27, 2008; Revised: June 28, 2009

Development of the positive temperature coefficient of resistivity (PTCR) in Er<sup>3+</sup> and Ca<sup>2+</sup> co-doped ferroelectric BaTiO<sub>3</sub> was studied in this work, with Er<sup>3+</sup> being used to act as a donor doping. Irrespective of all the materials showing high densities after sintering at 1200 to 1300 °C, these revealed insulator at the lowest sintering temperature, changing to semiconducting and PTCR-type materials only when the sintering temperature was further increased. Observations from X-ray diffraction help correlating this effect with phase development in this formulated (Ba,Ca,Er)TiO<sub>3</sub> system, considering the formation of initially two separated major (Ba,Ca)TiO<sub>3</sub>- and minor (Ca,Er)TiO<sub>3</sub>-based compounds, as a consequence of cation size-induced stress energy effects. Thus, appearance and enhancement here of the semiconducting and PTCR responses towards higher sintering temperatures particularly involve the incorporation of Er<sup>3+</sup> into the major phase, rendering finally possible the generation and “percolative-like” migration of electrons throughout the whole material.

**Keywords:** phase development, electrical properties, PTCR, BaTiO<sub>3</sub>

### 1. Introduction

Perovskite-structured ferroelectric BaTiO<sub>3</sub> has a relatively high tolerance for many cation dopants, which are normally used to engineer the electrical properties of the material. In this way, BaTiO<sub>3</sub> has found a number of electro-optic, electromechanical and dielectric applications<sup>1,2</sup>. Nevertheless, as recognized in literature, the largest commercial markets for this material seem to still be positive temperature coefficient resistors (PTCR) and multilayer capacitors (MLC)<sup>1</sup>. For these applications, the formulation often involves the incorporation of rare-earth cations into the host material<sup>3,4</sup>, the resulting electrical properties being strongly affected by the change in the occupational perovskite lattice sites. In particular, to induce n-type semiconductivity and PTCR behavior in BaTiO<sub>3</sub> ceramics, light doping of the material with donor-type tri- or penta-valent cations substituting, respectively, at the Ba<sup>2+</sup> (with a twelve-coordination number) or Ti<sup>4+</sup> (with a six-coordination number) sites is required<sup>4,5</sup>. Also, the ionic radius (IR) of the substituting element may strongly affect the incorporation site. For instance, ions with intermediate size like Er<sup>3+</sup> (1.00 Å)<sup>6</sup> can be accommodated at both Ba<sup>2+</sup> (1.61 Å)<sup>6</sup> and Ti<sup>4+</sup> (0.605 Å)<sup>6</sup> sites (called amphoteric effect), depending on doping concentration and stoichiometry of the hosting BaTiO<sub>3</sub> structure, according to literature<sup>3,7,8</sup>.

The study of defect chemistry of rare-earth cations in BaTiO<sub>3</sub> and, in particular, that of phase development and PTCR response of Er<sup>3+</sup>-doped BaTiO<sub>3</sub> have been achieved elsewhere<sup>3,7-9</sup>. Considering however that i) there are relatively few works dealing with rare earth-induced semiconductivity in BaTiO<sub>3</sub> in presence of co-doping cations taking effectively part of the bulk structure, and ii) a supposed right combination of host and doping elements may lead to the finding of optimized materials for the applications being envisaged, the purpose of the present work was the study of Er<sup>3+</sup>-induced semiconductivity and PTCR development in Er<sup>3+</sup> and Ca<sup>2+</sup> co-doped BaTiO<sub>3</sub> ceramics, with the particularity that the Ca<sup>2+</sup> co-dopant element shows as well

an intermediate ionic radius (1.34 Å)<sup>6</sup> not only between Ba<sup>2+</sup> and Ti<sup>4+</sup>, but especially also between Ba<sup>2+</sup> and Er<sup>3+</sup>. Through the achievement of structural measurements, differences in the electrical responses finally observed for these ceramics are discussed in terms of the distinct Ca<sup>2+</sup>-induced trends of phase formation during the sintering of such a co-doped material. In particular, the individual electrical properties of grains and grain boundaries versus phase development are also compared and correlated.

### 2. Experimental Procedure

Er<sup>3+</sup> and Ca<sup>2+</sup> co-doped BaTiO<sub>3</sub> ceramics were prepared through a polymeric precursor method, using high-purity titanium isopropoxide (Ti[OCH(CH<sub>3</sub>)<sub>2</sub>]<sub>4</sub>), barium acetate (C<sub>4</sub>H<sub>6</sub>BaO<sub>4</sub>), calcium carbonate (CaCO<sub>3</sub>) and erbium nitrate (Er(NO<sub>3</sub>)<sub>3</sub>·5H<sub>2</sub>O) as precursor materials. These raw materials were mixed, so as to nominally obtain the final composition Ba<sub>0.77</sub>Ca<sub>0.225</sub>Er<sub>0.005</sub>TiO<sub>3</sub>, calcined at 600 °C for 4 hours, and then sintered at 1200 and 1250 °C for 5 hours, and at 1300 °C for 1 hour. All the ceramic materials showed high densities, as reported in Table 1. X-ray diffraction (XRD) data of the specimens were collected at room temperature on a Rigaku Rotaflex RU-200B diffractometer, while scanning electron microscopy (SEM) observations were performed on a Zeiss® DSM960 equipment for evaluating the materials' average grain size (see final results also given in Table 1). Direct current (DC) and AC electrical measurements were carried out from room temperature to about 350 °C, using a 610C Keithley® electrometer and a Solartron® SI 1260 impedance/gain-phase analyzer (operative from f = 1 Hz to 13 MHz), respectively. The AC data were processed in terms of complex impedance [ $Z^* = Z' - jZ''$ ] and analyzed through the impedance/resistivity spectroscopy method<sup>10</sup>.

\*e-mail: peko@ifsc.usp.br

**Table 1.** Average density, grain size and room temperature grain, grain-boundary and total (grain plus grain-boundary) resistivity values processed for the Er<sup>3+</sup> and Ca<sup>2+</sup> co-doped BaTiO<sub>3</sub> samples.

Sintering Parameters	Density (% of TD)*	Grain size (μm)	Room temperature resistivity (Ω cm)		
			Grains	Grain bounds.	Total
1200 °C/5 hours	95.7	0.57	–	–	> 1.0 × 10 <sup>10</sup>
1250 °C/5 hours	98.7	1.02	2.0 × 10 <sup>6</sup>	4.2 × 10 <sup>6</sup>	6.2 × 10 <sup>6</sup>
1300 °C/1 hour	97.6	1.60	80.9	5.4 × 10 <sup>4</sup>	5.5 × 10 <sup>4</sup>

\* In percentage of Ba<sub>0.77</sub>Ca<sub>0.23</sub>TiO<sub>3</sub>'s theoretical density (TD = 5.55 g/cm<sup>3</sup>).

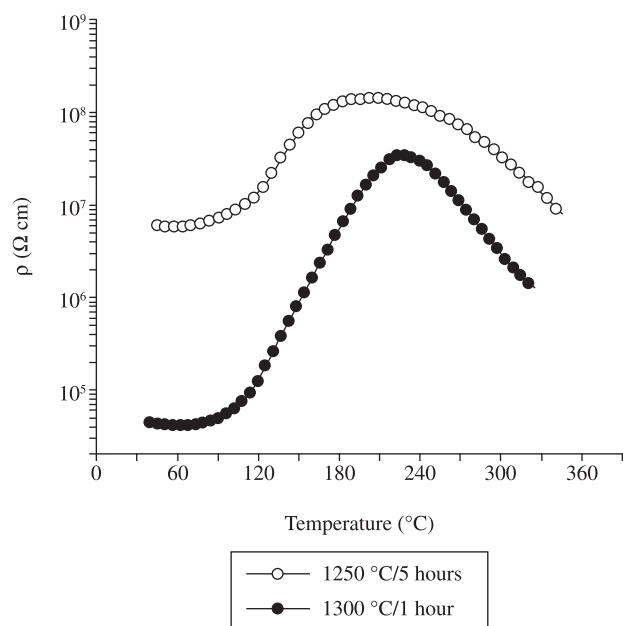
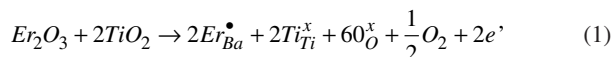


**Figure 1.** Temperature dependence of the DC resistivity measured on the Er<sup>3+</sup> and Ca<sup>2+</sup> co-doped BaTiO<sub>3</sub> samples sintered at 1250 °C for 5 hours and 1300 °C for 1 hour.

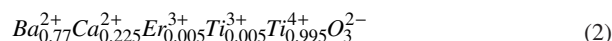
### 3. Results and Discussion

Figure 1 shows the temperature dependence of the DC resistivity ( $\rho$ ) for the materials sintered at 1250 °C/5 hours and 1300 °C/1 hour. A poor semiconducting appearance accompanied by a diffuse PTCR behavior are observed for sintering at 1250 °C/5 hours, characteristics that improve to a relatively high semiconductivity and proper PTCR effect for sintering at 1300 °C/1 hour. The room temperature (RT) resistivity for these latter sintering conditions is about two magnitude orders below that of the formers, while the corresponding resistivity jump (PTCR) parameter, defined here as  $\alpha = \rho_{\max} / \rho_{\text{RT}}$  is about 50 times higher, where  $\rho_{\max}$  refers to the maximum resistivity. The resistivity values observed in Figure 1 are comparable, in magnitude, with those wide-range values previously reported on 0.25 to 8 at. % Er<sup>3+</sup>-doped BaTiO<sub>3</sub><sup>7,9</sup>. According to literature<sup>3,7</sup>, both the nominal Ba/Ti molar ratio of R ( $\equiv 0.77$ ) < 1 and the low value of 0.5 at. % Er<sup>3+</sup> considered here should favor the preferential incorporation of Er<sup>3+</sup> at the Ba<sup>2+</sup> sites, leading to the electron compensation mechanism (Kröger and Vink notation):



and, thus, *n*-type semiconductivity and associated PTCR behavior generation in ferroelectric BaTiO<sub>3</sub> ceramics.

Still according to the DC measurements that were performed, the samples sintered at 1200 °C/5 hours were strongly insulator ( $\rho > 1.0 \times 10^{10} \Omega \text{ cm}$ ), as may also be deduced from the AC measurements subsequently conducted in this work. That is, Figure 2 depicts, in terms of  $\rho''$  vs.  $\rho'$  plots, the room temperature electrical features processed for the three sintering conditions. Figures 2b and 2c show the overlapping of two semicircles attributed to grains (towards the higher frequencies) and grain boundaries (towards the lower frequencies), that is, following the classical procedure of impedance/resistivity spectroscopy data analysis<sup>10</sup>. From this plotting formalism, each semicircle diameter basically reduces to the corresponding grain or grain-boundary resistivity, the results of which are also summarized in Table 1. Notice that, when compared to Figures 2b and 2c, the data from the samples sintered at 1200 °C/5 hours and shown in Figure 2a only suggest a quite higher resistivity, as a consequence of their still insulating character. At this point, from the electrical viewpoint at least, the trend of the higher sintering temperatures to be effectively inducing the formation of a Ba<sub>0.77</sub>Ca<sub>0.225</sub>Er<sub>0.005</sub>TiO<sub>3</sub>-like compound, as originally formulated, appears to be real, with its stoichiometry being in such a case interpreted as



In fact, we note that while the samples sintered at 1200 °C showed a pale-yellow color, this changed from grey-black to black with temperature increment from 1250 to 1300 °C, the dark color being associated with reduction of Ti<sup>4+</sup> to Ti<sup>3+</sup>, where



is the defect responsible for the appearance of semiconductivity and consequent observation of PTCR effect in ferroelectric BaTiO<sub>3</sub>-based ceramic materials.

To get further insight into these results, nevertheless, analysis of the materials' phase development through performing structural measurements was of great importance. Figure 3 shows the room temperature XRD patterns obtained for all the prepared ceramic samples. Reflection peaks isostructural with Ba<sub>0.88</sub>Ca<sub>0.12</sub>TiO<sub>3</sub> (JCPDS 81-1288) are observed, being accompanied by small, additional reflection peaks that were identified to be isostructural with CaTiO<sub>3</sub> (JCPDS 75-2100). The XRD intensity of this minor phase significantly decreases with increasing the sintering temperature, and tends in fact to disappear at 1300 °C. **With respect to these results, some observations are imperative to be made.** That is, results from our laboratory and current literature indicate that there is normally no second phase formation in sintered Ca<sup>2+</sup>-free Er<sup>3+</sup>-doped BaTiO<sub>3</sub>, excluding a minor Er<sub>2</sub>Ti<sub>2</sub>O<sub>7</sub> pyrochlore phase<sup>7</sup>, usually appearing for high Er<sup>3+</sup> doping contents, that is actually not found in the present work. Both this observation and Figure 3 therefore suggest that, during formation of Er<sup>3+</sup> and Ca<sup>2+</sup> co-doped BaTiO<sub>3</sub>, an intermediate stage involving the synthesis of an additional, minor (Ca,Er)TiO<sub>3</sub>-based compound is by some way energetically favored and forced to take place.

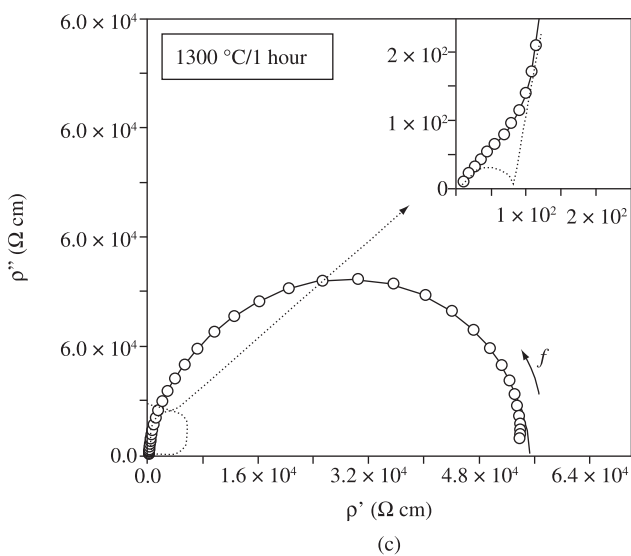
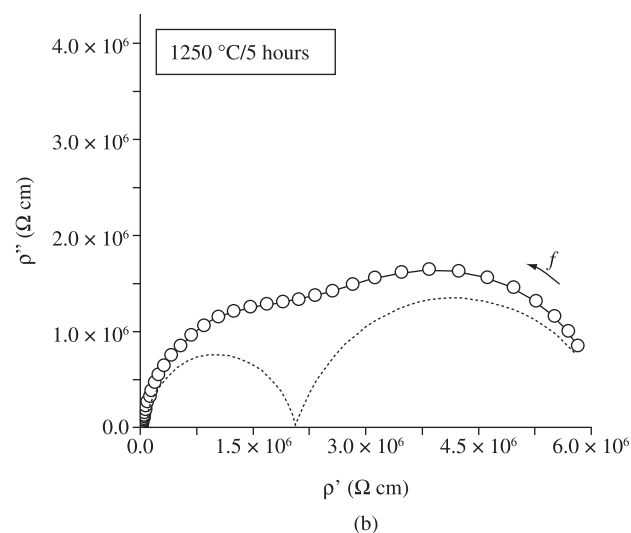
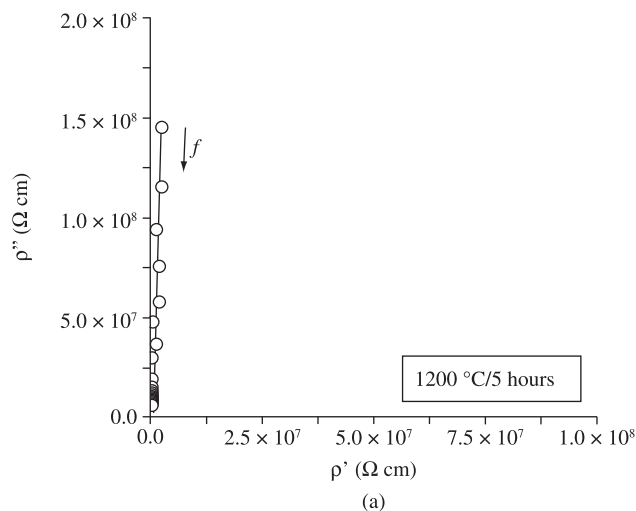


**Figure 2.** Room temperature complex resistivity spectra measured on the Er<sup>3+</sup> and Ca<sup>2+</sup> co-doped BaTiO<sub>3</sub> samples sintered at a) 1200 °C for 5 hours, b) 1250 °C for 5 hours and c) 1300 °C for 1 hour.

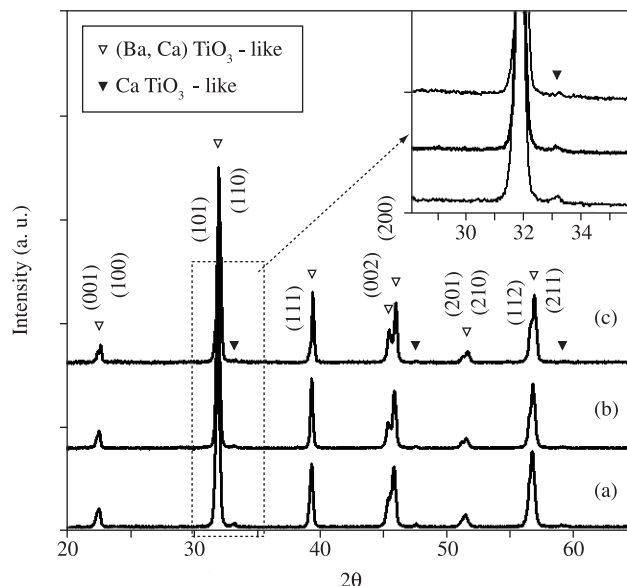


**Figure 3.** XRD patterns for the Er<sup>3+</sup> and Ca<sup>2+</sup> co-doped BaTiO<sub>3</sub> samples sintered at a) 1200 °C for 5 hours, b) 1250 °C for 5 hours and c) 1300 °C for 1 hour.

As from the electrical viewpoint the identical valence state of Ba<sup>2+</sup> and Ca<sup>2+</sup> theoretically implies equal probability (and no order) of Er<sup>3+</sup> to substitute for any of both cations at the perovskite A lattice sites, the above two-phase material formation in the early sintering stage should be understood in terms of stress energy effects during the simultaneous incorporation of Er<sup>3+</sup> and Ca<sup>2+</sup> into BaTiO<sub>3</sub>. For this particular case, notice that the ionic radius mismatches between foreign and host cations, with a different valence state, at the perovskite A sites are  $\Delta r(\text{Er}-\text{Ba}) = 0.61 \text{ \AA}$  and  $\Delta r(\text{Er}-\text{Ca}) = 0.34 \text{ \AA}$ . It is important to observe that the latter value really reveals quite lower in comparison. This makes reasonable to consider, as a reliable trend from the viewpoint of a partial, momentary reduction of internal lattice stresses, the simultaneous formation of initially a (Ca,Er)TiO<sub>3</sub>-based compound, besides the (Ba,Ca)TiO<sub>3</sub>-based one, as suggest the XRD results presented in Figure 3. Thereafter, still according to this figure, development of a solid-state reaction of both phases so as to give the formulated (Ba,Ca,Er)TiO<sub>3</sub> compound towards higher sintering temperatures may be assumed. We note that, like in this work, occurrence of an intermediate second phase formation during synthesis of BaTiO<sub>3</sub> co-doped with Y<sup>3+</sup> and Ca<sup>2+</sup> has also been inferred<sup>11</sup>. Although not explicitly mentioned, postulation of stress energy effects minimization should most likely also apply in that case.

In terms of correlation, in view of all the results presented and discussed above, the connection between phase development dynamics and the electrical properties that the sintered materials prepared here finally exhibited should be described as follows. First, Er<sup>3+</sup>-induced donor levels (associated with creation of the Ti<sup>3+</sup> defects) should initially form exclusively at the minor (Ca,Er)TiO<sub>3</sub>-type phase, with the observation that this phase does not percolate throughout the whole (composite-like) material, as this reveals insulator at 1200 °C (Figure 2a). At this stage, Ti<sup>3+</sup> defects could not migrate from the minor to the major (Ba,Ca)TiO<sub>3</sub>-like matrix provided that, while remaining free of Er<sup>3+</sup>, Ti<sup>3+</sup> would disturb electroneutrality requirement of this latter. Second, as the sintering temperature is further increased, reaching 1250 to 1300 °C, the Er<sup>3+</sup> cations are incorporated (via thermally-assisted ion diffusion) into the (Ba,Ca)TiO<sub>3</sub>-like matrix, where formation of Ti<sup>3+</sup>-associated donor levels would now take place,

rendering finally possible the “percolative-like” migration of electrons and, thus, semiconductivity and PTCR development throughout the whole material (Figures 1 and 2).

Further, achievement of the AC electrical measurements, whose results were presented in Figure 2 and summarized in Table 1, helps also showing and correlating how the electrical properties of these materials manifest at the microstructural (grain and grain-boundary) level during phase development. That is, looking at Table 1, the diminishing variation of the grain resistivity, from  $2.0 \times 10^6 \Omega \text{ cm}$  at  $1250^\circ\text{C}/5$  hours to  $80.9 \Omega \text{ cm}$  at  $1300^\circ\text{C}/1$  hour, supports the statement of a continuous thermally-assisted incorporation of  $\text{Er}^{3+}$  from the minor into the major  $(\text{Ba,Ca})\text{TiO}_3$ -based phase, resulting this matrix phase electronically compensated through the mechanism presented in reaction (1). The parallel decrease of the grain-boundary resistivity, from  $4.2 \times 10^6 \Omega \text{ cm}$  to  $5.4 \times 10^4 \Omega \text{ cm}$ , should result from i) a lesser (with respect to the grains) but also improved presence of  $\text{Ti}^{3+}$  defects at the matrix's grains surface, besides ii) the grain growth process (see results summarized in Table 1 in terms of grain sizes) that traduces, as well known, into a decrease of grain-boundary density in ceramic materials<sup>12</sup>.

According to Reference 7, finally, the increase of  $\text{Er}^{3+}$  into  $\text{BaTiO}_3$  (from 0.25 to 8 at. %) leads the material to gradually change from semiconductor to insulator, while the material's grain size continuously decreases ( $\text{Er}^{3+}$ -induced grain-boundary pinning effect), as in fact often found in several dopant-induced semiconductor  $\text{BaTiO}_3$  materials, see also e.g. Reference 13. In the present work, although postulating (with rising sintering temperature) the increasing incorporation of  $\text{Er}^{3+}$  into the  $(\text{Ba,Ca})\text{TiO}_3$ -based matrix, a fact of which justifies the generation and improvement of the materials' semiconducting and PTCR characters observed (Figures 1 and 2), the materials' grain size however also increased from sintering at  $1200$  to  $1300^\circ\text{C}$  (Table 1). This apparent contradiction, when compared with previous works as cited above, may be solved if considering that the secondary  $(\text{Er,Ca})\text{TiO}_3$ -based phase present at the lower sintering temperatures should be acting as an effective grain-boundary pinning and, thus, a grain-growth-inhibiting factor, that results much more important than the pinning effect expected from  $\text{Er}^{3+}$ .

It was shown in this work that synthesis of  $\text{Ba}_{0.77}\text{Ca}_{0.225}\text{Er}_{0.005}\text{TiO}_3$  ceramics is preceded by an intermediate stage involving the formation of a major  $(\text{Ba,Ca})\text{TiO}_3$ - and a minor  $(\text{Ca,Er})\text{TiO}_3$ -based phases, followed by the thermally-assisted solid-state reaction of both phases to give the final composition. This phase development feature may be accounted for considering a trend of stress energy minimization in the formulated system, because the higher ionic radius similarity between the  $\text{Er}^{3+}$  and  $\text{Ca}^{2+}$  dopant cations vs. the size mismatch between the  $\text{Er}^{3+}$  and host  $\text{Ba}^{2+}$  cations. Consequently, the expected semiconducting and PTCR behaviors of the  $(\text{Ba,Ca,Er})\text{TiO}_3$  materials only manifest and improve with increasing sintering temperature, a fact of which traduces into an effective thermally-assisted incorporation of  $\text{Er}^{3+}$  from the minor  $(\text{Ca,Er})\text{TiO}_3$ -based phase into the

major  $(\text{Ba,Ca})\text{TiO}_3$ -based one. In summary, both distinct phase development trend and sintering temperature-dependent electrical responses found in these  $\text{Er}^{3+}$  and  $\text{Ca}^{2+}$  co-doped  $\text{BaTiO}_3$  ceramics are to be viewed as a consequence of mixed dopant and host cations size effects.

## Acknowledgements

The authors gratefully acknowledge financial supports from FAPESP and CNPq, two Brazilian research-funding agencies.

## References

1. Moulson AJ and Herbert JM. *Electroceramics: Materials, Properties and Applications*. London: Chapman-Hall; 1990.
2. Jaffe B, Cook WR, and Jaffe H. *Piezoelectric Ceramics*. London: Academic Press; 1971.
3. Takada K, Chang E, and Smyth DM. *Advances in Ceramics*. JB Blum and WR Cannon (Eds.). *American Ceramic Society*. 1987; 19:147.
4. Kishi H, Kohzu N, Sugino J, Oshato H, Iguchi Y and Okuda T. The effect of rare-earth (La, Sm, Dy, Ho and Er) and Mg on the microstructure in  $\text{BaTiO}_3$ . *Journal of the European Ceramic Society*. 1999; 19(6-7): 1043-1046.
5. Heywang W. Semiconducting barium titanate. *Journal of Materials Science*. 1971; 6(9):1214-1226.
6. Shannon RD. Revised effective ionic-radii and systematic studies of interatomic distances in halides and chalcogenides. *Acta Crystallographica A*. 1976; 32:751-767.
7. Buscaglia MT, Viviani M, Buscaglia V, Bottino C and Nanni P. Incorporation of  $\text{Er}^{3+}$  into  $\text{BaTiO}_3$ . *Journal of the American Ceramic Society*. 2002; 85(6):1569-1575.
8. Tsur Y, Dunbar TD and Randall CA. Crystal and defect chemistry of rare earth cations in  $\text{BaTiO}_3$ . *Journal of Electroceramics*. 2001; 7(1):25-34.
9. Viviani M, Buscaglia MT, Buscaglia V, Mitoseriu L, Testino A, Nanni P and Vladikova D. Analysis of conductivity and PTCR effect in Er-doped  $\text{BaTiO}_3$  ceramics. *Journal of the European Ceramic Society*. 2004; 24(6):1221-1225.
10. García-Sánchez MF, M'Peko JC, Ruiz-Salvador AR, Rodríguez-Gattorno G, Echevarría Y, Fernández-Gutierrez F and Delgado A. An elementary picture of dielectric spectroscopy in solids: Physical basis. *Journal of Chemical Education*. 2003; 80(9):1062-1073.
11. Belous AG, V'yunov OI, Kovalenko LL, Buscaglia V, Viviani M, and Nanni P. Effect of isovalent Ba-site substitutions on the properties of  $(\text{Ba}_{1-x-y}\text{M}_y\text{Y}_x)\text{TiO}_3$  (M = Ca, Sr, Pb) PTCR ceramics. *Inorganic Materials*. 2003; 39(2):133-138.
12. Verkerk MJ, Middelhuis BJ and Burggraaf AJ. Effect of grain-boundaries on the conductivity of high-purity  $\text{ZrO}_2\text{-Y}_2\text{O}_3$  ceramics. *Solid State Ionics*. 1982; 6 (2):159-170.
13. Ting CJ, Peng CJ, Lu HY and Wu ST. Lanthanum-magnesium and lanthanum-manganese donor-acceptor-codoped semiconducting barium titanate. *Journal of the American Ceramic Society*. 1990; 73(2):329-334.